academicJournals

Vol. 13(7), pp. 844-856, 12 February, 2014
DOI: 10.5897/AJB2013.13078
ISSN 1684-5315 ©2014 Academic Journals
http://www.academicjournals.org/AJB

African Journal of Biotechnology

Full Length Research Paper

AtNEA1-identification and characterization of a novel plant nuclear envelope associated protein

Ting Lu

Department of Biological and Medical Sciences, Oxford Brookes University, Oxford OX3 0BP, UK.

Accepted 29 January, 2014

In animal and yeast cells, a cross nuclear envelope structure linker of nucleoskeleton and cytoskeleton (LINC) is formed by outer nuclear membrane SUN proteins and inner nuclear membrane KASH proteins. However, little information was acquired about plant SUN-KASH structure until they were found in plant SUN proteins in 2010 and KASH proteins in 2012. The SUN-KASH complex alongside with actin in the microfilament cytoskeleton and nucleaoskeleton together shape the main cell skeleton structure and involve in many important biological functions including cell structure stability, cell movement and cell division. In searching of other plant nuclear envelope associated proteins, arabidopsis nuclear envelop associated (AtNEA1) protein 1, a plant nucleoplasmic protein, was identified from biological studies. AtNEA1 was predicted to have a nuclear localisation signal (NLS), two coiled coil domains and one transmembrane (TM) domain. The mutants with the deletion of respective putative domains were observed under confocal microscopy. The subcellular localisation of mutants implied that putative NLS is not essential for AtNEA1 to diffuse through NPC but can strongly increase the efficiency, both coiled coil domains participate in the interaction of AtNEA1 with its unknown INM intrinsic interaction partner, and putative TM appeared to be non-functional. The function of AtNEA1 in plant was studied through observing tDNA lines.

Key words: Arabidopsis nuclear envelope associated protein 1 (AtNEA1), bioinformatics search, confocal microscopy, nucleoplasmic protein, domain deletions, truncation.

INTRODUCTION

The Nuclear Envelope (NE) consists of an inner nuclear membrane (INM) and an outer nuclear membrane (ONM). The pore membrane accommodates the nuclear pore complex (NPC) and connects INM and ONM (Evans et al., 2004, 2011; Fiserova et al., 2009). The ONM is also connected with the endoplasmic reticulum (ER), and hence; allows the NE to function with the endomembrane network (Crisp and Burke, 2008; Razafsky and Hodzic, 2009). The INM and ONM contain a series of proteins and these proteins execute important cellular functions. A number of proteins of the INM are associated with the nuclear lamina - a protein meshwork composed of lamins. The nuclear lamina attaches chromatin to the NE and stabiles the structure of nucleus. The ONM proteins together with cytoskeletal components function in cell movement and nuclear positioning. Anchored to the nuclear pore membrane is the nuclear pore complex (NPC), which has a framework of a central gated channel with cytoplasmic and nuclear filaments. The NPC facilitates the exchange of macromolecules (RNA, proteins, carbohydrates and lipids) between cytoplasm and nucleus (Doye and Hurt, 1997; D'Angelo and Hetzer, 2006; Stewart et al., 2007; Meier and Brkljacic, 2009a).

The INM can connect to chromatin directly and through the lamina. The nuclear lamina is a meshwork of about 10 to20 nm thick and is formed by lamins and

E-mail: tlu.at.brookes@gmail.com.

lamin-associated proteins (Gruenbaum et al., 2005; Stewart et al., 2007; Prokocimer et al., 2009). The nuclear lamina helps to support the structure of the nucleus in terms of providing a framework at the INM and is involved in various cellular processes including mitosis and nuclear activities (Broers et al., 1999; Gruenbaum et al., 2005; D'Angelo and Hetzer, 2006; Prokocimer et al., 2009). The nuclear lamins are type V intermediate filaments. The IF has a tripartite structure, which is shaped by a helical rod domain in the centre with a short head domain and a long tail (Prokocimer et al., 2009). Four coiled coils form the centre rod domain and they are linked by a linker structure (Stuurman et al., 1998; Herrmann and Aebi, 2004). The linkage from cytoskeletal elements to INM proteins, from INM proteins to lamins, and from lamins to nucleoskeleton and chromatin forms a bridge across the nuclear envelope to participate in cellular processes like mitotic spindle assembly, nuclear positioning and cell movement. In addition, lamins participate in gene transcription activities through interaction with BAF, RNA and other transcriptional regulators (Goldberg et al., 1999). The lamins interact with proliferating cell nuclear antigen (PCNA) protein, chromatin and DNA matrix attachment region (MAR) to support the scaffold for DNA replication.

MAR are specific DNA sequences functioning in maintaining and mediating chromatin structure in the regulation of gene expression (Moir and Spann, 2001; Vlcek et al., 2001; Gruenbaum et al., 2005; D'Angelo and Hetzer, 2006). An important INM protein family is the SUN (Sad1/Unc-84) domain protein family. SUN domain proteins consist of an N-terminal nucleoplasmic portion and at least one transmembrane domain embeded in the INM. The nucleoplasmic portion of SUN domain proteins interact with nucleoskeletal components like type-A and type-B lamins (Hodzic et al., 2004; Haque et al., 2006; Tzur et al., 2006; Wang et al., 2006). The regulation of interactions between lamins and SUN domain proteins is largely unknown (Razafsky and Hodzic, 2009). The C-terminal portion of SUN domain proteins is in the lumen and interacts with KASH domain proteins. KASH domain proteins are a major family of ONM-intrinsic proteins in animal and yeast cells (Wilhelmsen et al., 2006). The interaction of SUN domain proteins and KASH domain proteins forms the linker of nucleoskeleton and cytoskeleton (LINC) complex, which provides a physical connection across the NE (Crisp et al., 2006). It is crucial for the duplication of centrosomes and spindle pole bodies (SPB) at NE, and formation anchorage of the chromosome bouquet in mitosis. The LINC complex is also important for spanning the width of the nuclear periplasm (approximately 30 to 50 nm) (Chikashige et al., 2006; Crisp et al., 2006; Tomita and Cooper, 2006; Tzur et al., 2006; Chi et al., 2007; Kemp et al., 2007; Starr, 2009; Graumann et al., 2010). Some INM proteins take part in biochemical signaling in the nucleus. MAN1 contains a LEM domain and the C-terminus of MAN1 binds to Smad proteins, which are receptor-regulated (Massague et al., 2005).

The Smad proteins then mediate downstream signaling of TGF-β superfamily including bone morphogenetic protein (BMP) signaling (Osada et al., 2003; ten Dijke and Hill, 2004; Lin et al., 2005). Human MAN1 binds to Smad2 and Smad3 and antagonizes signaling by transforming growth factor-β (TGF-β) (Gruenbaum et al., 2005; Lin et al., 2005). In yeasts, INM proteins amino acid sensor independent (Asi)1, Asi2 and Asi3 function as negative regulators of Ssy1-Ptr3-Ssy5 (SPS) sensor signaling. The SPS sensor regulates the activity of transcriptional factors Stp1 and Stp2, which are synthesized as latent cytoplasmic factors (Forsberg and Ljungdahl, 2001; Andreasson and Ljungdahl, 2002). Emerin is associated with the death promoting factor Btf, the splicing associated factor YT-521B and the transcriptional repressor germ cell less (GCL) (Holaska et al., 2003; Wilkinson et al., 2003; Haraguchi et al., 2004). GCL and BAF compete *in vitro* to bind with emerin (Holaska et al., 2003). BAF recruits emerin to chromatin in nuclear assembly in animal cells. The recruitment is crucial for emerin to be localized at the reformed NE (Haraguchi et al., 2001; Holaska et al., 2003). In animal cells, SUN1/matefin is the pro-apoptotic Ced4 receptor and is required for programmed cell death (Tzur et al., 2006). LBR is another vital INM proteins which was first identified in 1988 (Worman et al., 1988). It contains an N-terminal nucleoplasmic portion of 210 amino acids forming two globular domains, a C-terminal hydrophilic domain and 8 transmembrane domains (Worman et al., 1988; Chu et al., 1998). The independent hinge region of LBR binds to chromatin (Ye et al., 1997). The binding is mediated by heterochromatin protein (HP1). The second globular domain of LBR binds to HP1 and the interaction between LBR and HP1 is involved in vesicle targeting to chromosomes at the end of mitosis (Pyrpasopoulou et al., 1996; Buendia and Courvalin, 1997; Ye et al., 1997). In human cells, LBR antibody can also detect lamin B, implying interaction between LBR and lamina (Lassoued et al., 1991; Lin et al., 1996). The interaction of LBR and the lamina supports the attachment of the lamina to the INM and stabiles the NE structure. Figure 1 illustrates the overview of the nucleus and INM proteins. Mutations in emerin and LBR cause diseases (Morris, 2001; Hoffmann et al., 2002; Waterham et al., 2003).

Other typical plant nuclear proteins include MAR-binding filament like protein 1 (MFP1), MAR-binding filament like protein 1 associated factor 1 (MAF1), filament-like plant proteins (FPP), nuclear intermediate filament (NIF) and nuclear matrix protein 1 (NMP1) (Meier et al., 1996; Gindullis et al., 1999, 2002; Rose et al., 2003; Blumenthal et al., 2004). MFP1 functions to connect chromatin to the nuclear lamina and is considered as the homologue of MAR-binding proteins in animal cells (Harder et al., 2000). MAF1 is the MFP1 binding partner in plants. It consists of a WPP (tryptophan-

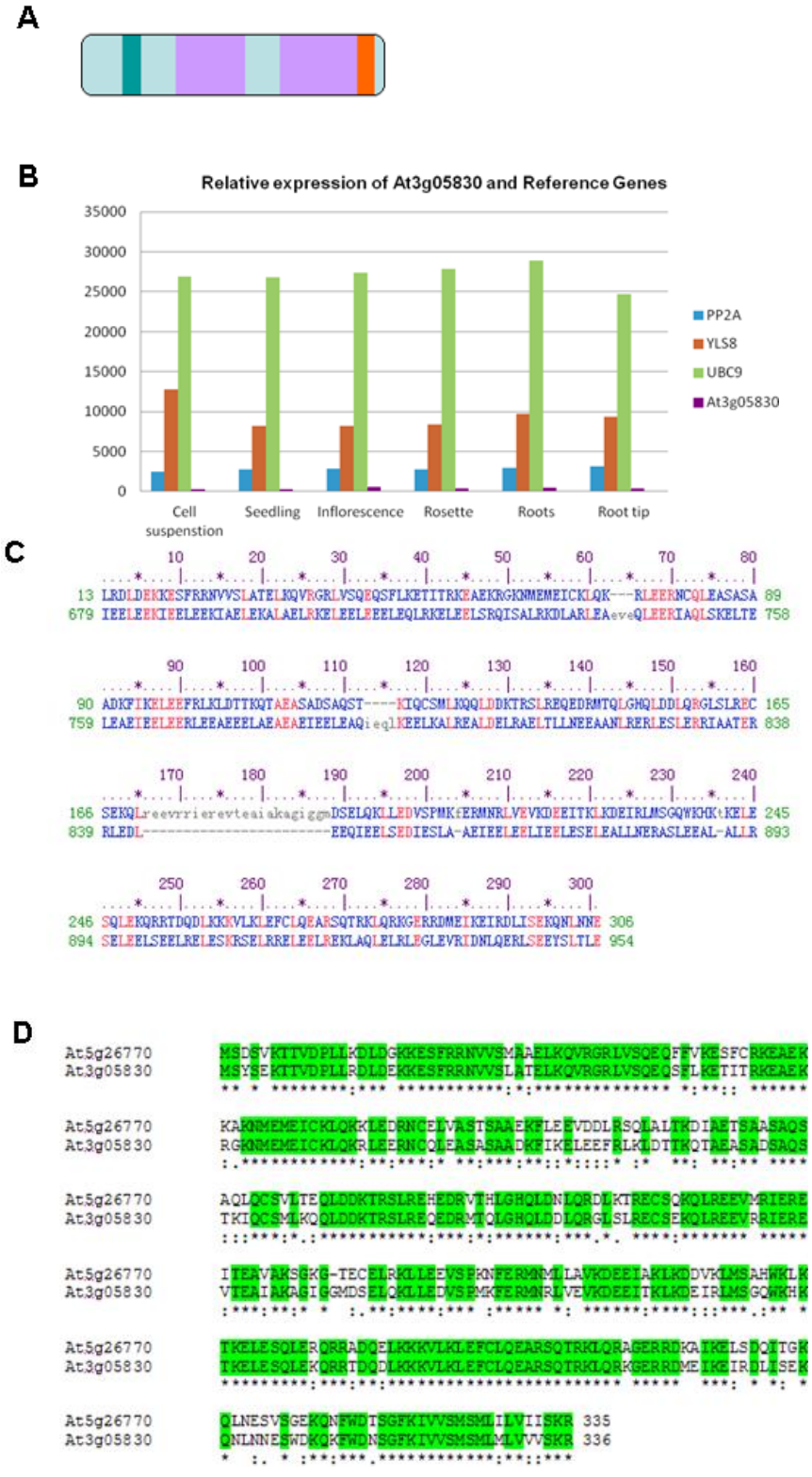

Figure 1. Bioinformatics information of At3g05830 (AtNEA1). Bioinformatics searches were conducted and the relevant information is shown as: (A) Domain structure prediction of At3g05830, cyan: bipartite nuclear localization signal (NLS), purple: coiled coil domains, orange: putative transmembrane domain, location and size of domains were determined by SMART and MotifScan facilities. (B) The relative expression pattern of At3g05830 in *A. thaliana* from Genevestigator. Reference genes: blue: Protein phosphatase 2A subunit-PP2A (At1g13320); red: Yellow leaf-specific protein 8-YLS8 (At4g27960); green: Ubiquitin conjugating enzyme-UBC9 (At4g27960): mauve: At3g05830. (C) The structure alignment of At3g05830 with a typical SMC protein SMC_prok_B (TIGR02168) from NCBI CDD facility. (D) The DNA alignment of At5g26770 with At3g05830 from NCBI BLAST facility.

proline-proline) domain and is unique to plants (Gindullis et al., 1999; Patel et al., 2004; Rose et al., 2004). FPP is also exclusive to plants and interacts with MAF1. NIF is a sequence homologue to lamins in animal cells. NMCP1 is conserved in plants and is located at nucleus (Gindullis et al., 2002; Rose et al., 2003; Blumenthal et al., 2004). LITTLE NUCLEI 1 (LINC1) and LINC2 proteins are two important plant nuclear proteins. LINC1 is localized to the nuclear periphery and LINC2 is localized to the nucleoplasm (Dittmer et al., 2007). LINC1 and LINC2 are NMCP1 homology proteins in arabidopsis. The deletion of either LINC1 or LINC2 causes nucleus size reduction and nuclear morphology change. The deletion of both genes causes not only nuclear shape alteration but also chromocenter number reduction and whole-plant morphology dwarfing (Dittmer et al., 2007). In addition to LINC1 and LINC2, LINC 3 was identified as a nucleolar protein and LINC4 was identified as a plastid protein (Kleffmann et al., 2006; Pendle et al., 2005).

One of the potential plant NE specific proteins is DMI1 (does not make infection 1). DMI1 responds to Nod factor signaling which is released by nitrogen-fixed bacteria to participate in generating perinuclear calcium oscillations (Peiter et al., 2007; Riely et al., 2007). Ran GTPase activating protein (RanGAP) has also been found in the plant ONM (Meier et al., 2010).

The anchoring of plant microtubules to the NE is through the interaction of γ-tubulin ring complexes (γ-TuRC) with plant gamma-tublin complex proteins (GCP) AtGCP2 and AtGCP3. The NE localization domains of AtGCP2 and AtGCP3 can interact with ONM intrinsic proteins, anchoring γ-TuRC to the plant NE (Seltzer et al., 2007). The nuclear calcium level is regulated by calcium channels and pumps located in both INM and ONM (Xiong et al., 2006). A lycopersicon Ca^{2+} ATPase (LCA) in tomato cells is a homologue of the SERCA calcium pump found at the NE in plants (Downie et al., 1998). DMI1 is essential for calcium spiking through the conductance of a K+ (RCK) domain at its C-terminus (Peiter et al., 2007; Riely et al., 2007). Both DMI1 and LCA were shown at the NE by confocal and electron microscopy using immunofluoresence labeling or immunogold labeling (Riely et al., 2007). RanGAP is anchored to the ONM and is crucial for NPC transport, SPB assembly and NE reformation after cell mitosis (Xu and Meier, 2008; Zhao et al., 2008). Plant RanGAP has a unique WPP domain, which is important for RanGAP localization at ONM (Meier, 2007). Although, similarities do exist, significant differences have been found between plant cell nuclei and those of animals or yeast cells.

For example, no lamin sequence homologues have been identified in the plant cell nucleus (Graumann and Evans, 2010; Goldberg et al., 1999; Meier, 2001). However, a lamin-like protein nuclear matrix constituent protein 1 (NMCP1) can be detected using anti-lamin antibodies (Li and Roux, 1992; McNulty and Saunders, 1992; Masuda et al., 1997; Meier, 2007). NMCP1 has a structure of a coiled coil domain, α-helix and a nuclear localization signal (NLS). NMCP1 contains phosphorylation sites for kinases as well. These characteristics imply NMCP1 is a lamin substitute in plant (Masuda et al., 1997).

The aim of the project was to identify potential novel NE or NE-associated proteins in plants and to characterise them. Arabidopsis nuclear envelope protein 1 (AtNEA1), was probed as a plant nuclear envelope associated protein, which is anchored to the INM by interacting with an unknown interacting partner. The subcellular localization of AtNEA1 was identified by approaching *in vivo* fluorescence transient expression as well as BY-2 cells stable expression observed by confocal microscopy. The function of AtNEA1 was probed by applying tDNA mutant lines study and BY-2 cell stable expression study. The novel discovery of AtNEA1 has boarded the view of plant nuclear envelope (NE) structure and NE associated proteins.

MATERIALS AND METHODS

Bioinformatics

The accesses Pfam, Sanger, Aramemnon and Interpro predictive protein and pattern database (http://pfam.sanger.ac.uk/search?tab=searchSequenceBlock; http://smart.embl-heiderberg.de; http://aramemnon.botanik.uni-koeln.de/index.ep; http://www.ebi.ac.uk/interpro) were used to select At3g05830 (in this study, At3g05830 refers to At3g05830.1 subtype) as putative KASH-like gene in arabidopsis. The amino acid sequence of At3g05830 was compared with amino acid sequences in EXPASY, NCBI BLAST and NCBI CDD accesses (http://expasy.org/; http://blast.ncbi.nlm.nih.gov/Blast.cgi; http://www.ncbi.nlm.nih.gov/cdd) to investigate DNA and structural homologues. Relative expression data for AtNEA1 and reference genes were obtained from the genevestigator database (http://www.genevestigator.ethz.ch/).

Cloning and transient expression of AtNEA1 in *Nicotiana benthamiana*

The gene encoding At3g05830 (AtNEA1) was fused into donor vector pDONR207 (Invitrogen, Paisley, UK) by the Gateway BP reaction. YFP fused expressions vector pCAMBIA-YFP-casA and pCAMBIA-casB-YFP (Invitrogen, Paisley, UK) encoding AtNEA1 were gained by the Gateway LR reaction. Built up expression vectors were transfected into *Agrobacterium tumefaciens* strain GV3101 (Koncz and Schell, 1986). Bacterial cells were resuspended in infiltration buffer [0.5% (w/v) glucose, 50 mM MES, 2 mM trisodium phosphate, 100 µM acetosyringone, pH 5.6]. For transformation, *A. tumefaciens* cells containing YFP- tagged expression vectors were adjusted to a D_{600} = 0.4 ratio and infiltrated in 5 week old *N. benthamiana* leafs. Infiltrated *N. benthamiana* leafs were cropped and observed 72 h after transformation.

Cloning, expression and purification of AtNEA1 in *Escherichia coli*

The gene encoding AtNEA1 was amplified from a cDNA library obtained by RT-PCR from cauline leafs of *A. thaliana* and cloned

into the expression vector pDONR207 (Invitrogen, Paisley, UK). The gained vector was transfected into the *E. coli* strain DH5α and cells were grown in LB [1% (w/v) bacto-tryptone, 0.5% (w/v) bacto-yeast extract, and 1% sodium chloride] medium at 37°C. Cells were harvested 12 h after induction and the vectors were purified. For purification of pDONR207-AtNEA1, cells were pelleted and resuspended in 250 µl resuspension solution (Promega, Southampton, UK). The same amount of cell lysis solution (Promega, Southampton, UK) was added to mix. 10 µl alkaline protease solution (Promega, Southampton, UK) was added to mix. 350 µl neutralization solution was added to mix. After centrifugation of the cell lysate at 140 00 *g*, the supernant was decanted into the spin column. 750 µl wash solution (Promega, Southampton, UK) was added and the collection tube (Promega, Southampton, UK) was centrifuged at 140 00 *g*. The wash was repeated once with 250 µl wash buffer. The DNA was eluted in 40 µl nuclease free water and the sequence was analyzed by gene sequencing.

Confocal microscopy

Confocal microscopy was conducted by a Zeiss LSM 510 Laser Scanning Microscopy (Carl Zeiss GmbH, Hertfordshire, UK) with a Plan-Neoflur 63 × / 1.4 oil immersion objective. The following settings were used throughout the experiments: YFP excitation 514 nm, CFP excitation 458 nm, detection wavelength 530 to 600 nm for YFP and 475 to 525 nm for CFP. Images were processed using Zeiss LSM 510 Software (Carl Zeiss GmgH, Hertfordshire, UK). For fluorescence resonance energy transfer (FRET) interaction studies, YFP- and CFP- tagged expression vectors encoding for AtNEA1 and AtSUN1/AtSUN2 were co-infiltrated in *N. benthamina*. FRET was measured with the acceptor bleaching method. The acceptor YFP was bleached 10 times with 100% laser power of the 514 nm diode laser line in a region of interest (ROI). FRET was quantified by measuring CFP fluorescence intensity in the bleached area before (5 frames) and after (10 frames) bleaching. FRET efficiency ($FRET_{eff}$), which is the percentage fluorescence intensity, was calculated according to the following expression:

$$FRET_{eff} = \{(I\ [CFP_{after\ bleaching}] - I\ [GFP_{before\ bleaching}] / I\ [GFP_{after\ bleaching}])\} \times 100$$

The test of AtNEA1 solubility *in vivo*

Transiently YFP- tagged AtNEA1 transformed leaf tissue was crushed on ice with 50 µl exaction buffer (10 mM Tris HCl, 150 mM NaCl, 0.5 to 1.0% Triton X-114). After centrifugation at 140 00 *g* at 4°C, supernatant was decanted to a fresh eppendorf tube and brought up to 250 µl with extraction buffer. Protein sample was gently overlaid on 300 µl sucrose cushion (6% sucrose, 10 mM Tris HCl, 150 mM NaCl, 0.06% Triton X-114). Samples were centrifuged at 300 *g* at 30°C (Sorvall, Bishop's Stortford, UK) after 3 min incubation at 30°C. Upper aqueous phase was decanted into a fresh eppendorf tube. The lower detergent phase was overlaid on the sucrose cushion for 3 min incubation at 30°C followed by 3 min centrifugation at 30°C. The supernatant was discarded. The aqueous phase was rinsed with 2% concentrated Triton X-114. Both aqueous phase and detergent phase were brought up to the equal volumes as well as concentrations of salt and surfactant. Bovine serum albumin (10 mg/ml) was added to samples in a ratio of 3%. 1.5 m^3 of saturated ammonium sulphate solution was added and mixed. The tubes were incubated for 2 h followed by 10 min full speed centrifugation at 4°C. The supernatant was discarded.

Buffer TE (50 mM Tris, 2 mM EDTA) was added to the pellets in a ratio of 20% and the samples were incubated on ice for 30 min. Samples (both aqueous phase and detergent phase) were analyzed by SDS-PAGE gel followed by Western blot (Bordier, 1981).

Domain deletions and truncation

The bioinformatics study predicted 4 putative functional domains in AtNEA1 (SMART: http://smart.embl-heidelberg.de/ and MotifScan: http://myhits.isb-sib.ch.cgi-bin/motif_scan). They are: putative nuclear localization signal (NLS) - from 60 to 75 amino acids; coiled coil 1 - from 121 to 180 amino acids; coiled coil 2 - from 238 to 306 amino acids; putative transmembrane domain - 321 to 334 amino acids. By adopting splicing by overlapping extension (SOE) PCR protocol (Dahm and Jennewein, 2010), the putative NLS and coiled coil domains were deleted and putative transmembrane domain was truncated (the last two amino acids were removed from the gene as well). The mutants were fused into pCAMBIA- YFP vectors by Gateway protocol and transiently expressed in *N. benthamiana* at a D_{600} = 0.4 ratio. The infiltrated leafs were observed by confocal microscopy 72 h after transformation.

SAIL_SALK T-DNA lines

Six arabidopsis agar medium plates [2.2 g/l M&S media (Sigma M0404), 0.5 g/l MES, pH 5.7, 0.6% agar] were prepared under sterile conditions, half of the plates with kanamycin (10 mg/l) and the other half without. A small quantity of seeds - wild type (provided from this lab), SAIL line-SAIL_846_B07.v1 (N837770) (NASC, Nottingham, UK) and SALK line -SALK_021615.44.45.x (N521615) (NASC, Nottingham, UK) were placed into respective 1.5 ml Eppendorf tube. The bleach solution (10% NaClO; 0.02% Tween-20) was added and the tubes were shaken. The tubes were laid in laminar flow hood for 10 min to let the seeds precipitate to the bottom of tube. The supernatant was decanted and the bleach solution was added again. The wash was repeated 3 times. The seeds were resuspended in 500 µl dH_2O. The resuspended seeds were aliquoted onto a filter paper. The seeds were picked and dropped onto agar plates by using a sterile cocktail wooden stick. The plates were sealed with semi-permeable tape. The plates were wrapped with foil and stored at 4°C for 2 days to stratify, the plates were taken out, the foil was removed and the plates were incubated at 28°C in a culture room.

T-DNA line nucleus size measurements

Seedlings (14 day old) showing the same development stage were placed in 6.252 mg/ml ethidium bromide for 16 min at room temperature. Fluorescence of the nucleus of the leaf tissues were observed by laser scanning confocal microscopy to measure the size of the nucleus. Images were taken in the focal plane where the nucleus diameter was largest and then, the surface of this section was measured using ZEISS LSM image browser software. The settings for confocal microscopy were 514 nm excitation wavelength, ×40 objective lense, beam splitters: HFT 458-514, NFT 515, channel: Ch2, filter: BP560-615. The data was analysed by F-test followed by the student t-test with 5% significance level probability.

T-DNA line genotype examination

Leaf tissue was punched out by closing a microfuge lid on the leaf. The leaf material was ground in the microfuge using a disposable pestle for 15 s without buffer. 400 µl extraction buffer was added at room temperature, the microfuge was vortexed for 5 s. The samples were left at room temperature for 1 h. The sample was centrifuged (Beckman Coulter, High Wycombe, UK) at 13000 rpm for 1 min. Supernatant (300 µl) was added to 300 µl isopropanol at room temperature. The samples were left at room temperature for 2 min. The samples were centrifuged (Beckman Coulter, High Wycombe,

UK) at 13000 rpm for 5 min to pellet the DNA. Isopropanol was removed and the pellets were dried in a speed-vac. The DNA was resuspended in 100 µl sterile water. All the sample DNA was set in 4 PCR reactions with primers of T-DNA insertion - PCR reaction 1: SALK left primer (LP)*: 5' - AAT TTC TGG TCG AAT GCA TTG - 3', SALK right primer (RP)*: 5' - CCT GAA GAC GAC ACA TAC ATG AG - 3'; PCR reaction 2: SAIL left primer (LP)*: 5' - CTC TGC AGC TTT CTT GTC TGG - 3', SAIL right primer (RP)*: 5' - AGC TTG AAG CTT CTG CAT CTG - 3'; PCR reaction 3: LBb1.3*: 5' - TAA AAC GGC TAA AGC CTT G - 3', SALK right primer (RP)*: 5' - CCT GAA GAC GAC ACA TAC ATG AG - 3'; PCR reaction 4: LBb1.3*: 5' - TAA AAC GGC TAA AGC CTT G - 3', SAIL right primer (RP)*: 5' - AGC TTG AAG CTT CTG CAT CTG - 3'. LP (SAIL), RP (SAIL), LP (SALK), RP (SALK), LBb1.3 sequence information was obtained from SIGNAL: http://signal.salk.edu/T-DNAprimers.2.html.

The primers were ordered from Invitrogen (Paisley, UK). The PCR products were examined using DNA agarose gel.

BY-2 cells synchronisation and study

7 ml of 7-day old BY-2 cells (transformed with AtNEA1-YFP and YFP-AtNEA1) were transfered into 50 ml fresh BY-2 medium and 50 µl 5 mg/ml aphidicolin was added. The culture was incubated at 130 rpm, 27°C for 24 h. Cells were washed with 10 × 50 ml fresh BY-2 medium in a scintered funnel. Cells were resuspended in 50 ml fresh BY-2 medium and returned into incubator. Cells were observed with confocal microscopy.

RESULTS

Bioinformatics

To select the potential KASH-like proteins in plants, the conserved domain features (actin-binding domain, coiled coil domain and transmembrane domain) of KASH proteins were used as the query in a protein BLAST search, in which At3g05830 (one NLS, two coiled coils and one putative transmembrane domain) was selected as potential KASH-like protein in plants. At3g05830 is 336 amino acids long, with predicted molecular mass of 39.58 kDa. The predicted NLS (amino acids 60 to 75), coiled coil 1 domain (amino acids 121 to 180), coiled coil 2 domain (amino acids 238 to 306) and transmembrane domain (amino acids 321 to 334) are shown in Figure 1A. The *in vivo* expression pattern for At3g05830 in *A. thalianas* (Genevestigator: http://www.genevestigator.ethz.ch/) shows At3g05830 is universally expressed in a relative very low manner. But the expression level in embryonic system is comparably higher than other systems, suggesting its involvement in development. Figure 1B shows the relative expression pattern of At3g05830 in *A. thaliana*s. The structure study (NCBI CDD: http://www.ncbi.nlm.nih.gov/cdd) showed At3g05830 matches structural features of structural maintenance of chromosomes (SMC) protein family, suggesting its potential function in regulating the structure and organization of chromosomes. Figure 1C shows the alignment of At3g05830 with typical SMC protein: SMC_prok_B (TIGR02168).

The DNA homology search (NCBI BLAST: http://blast.ncbi.nlm.nih.gov/Blast.cgi) for At3g05830 indicated very low similarity in animal and yeast cells from searching but has one highly matching (81%) homologue in plant (At5g26770: an uncharacterized protein). Figure 1D shows the DNA alignment of At3g05830 with At5g26770. This fact indicates that At3g05830 may be plant conserved.

Subcellular localization of the YFP- tagged AtNEA1

To identify the subcellular localization of AtNEA1, a full-length form of AtNEA1 fused to YFP at the N- and C-terminal were constructed and transiently expressed in *N. benthamiana*. Expression of the fluorescent AtNEA1 fusion vectors were examined by confocal microscopy. As shown in Figure 2, the fluorescence signals emitted concentrate at the nuclear envelope periphery region. The identity of the stained pattern and the subcellular localization was demonstrated by co-expression of the CFP- labeled NE marker AtSUN1. The perfect overlay of both expression patterns shown in Figure 2C demonstrate the co-localization of both proteins and verified localization of AtNEA1 at the NE periphery.

Test of AtNEA1-AtSUN1 and AtNEA1-AtSUN2 interactions via FRET microscopy

FRET was adopted to test the potential interactions of AtNEA1 with AtSUN1 or AtNEA1 with AtSUN2 using the fluorophores YFP as donor and CFP as acceptor. The acceptor fluorophor was fused to the N- and C- terminus of AtSUN1 and AtSUN2, whereas the donor was attached to the N- and C- terminus of AtNEA1. *N. benthamiana* leaf cells were co-transformed with both vector constructs and the leaf samples were fixed by latrunculin B (Caorsi et al., 2011). Upon excitation of doubly transformed leaf cells at 514 and 458 nm, both YFP and CFP showed clear fluorescence. However, the statistic calculation did not indicate interactions between AtNEA1 with either AtSUN1 or AtSUN2 upon bleaching. The FRET statistic data table is shown in Table 1. The CFP fluorescence did not increase upon acceptor bleaching. Control experiments were carried out by CFP- tagged AtSUN1 or AtSUN2. No significant increase ($p<0.05$) of CFP fluorescence after YFP photobleaching is observed. The same information is gained by FRET of AtNEA1-YFP with CFP-tagged AtSUN1 or AtSUN2.

The solubility test of AtNEA1 from *N. benthamiana* transiently expression

Fused YFP-AtNEA1 and AtNEA1-YFP constructs were transiently expressed in *N. benthamiana* leafs (infiltrated at a ratio of $D_{600} = 0.4$). The expression was examined by confocal microscopy observe. The infiltrated leafs were

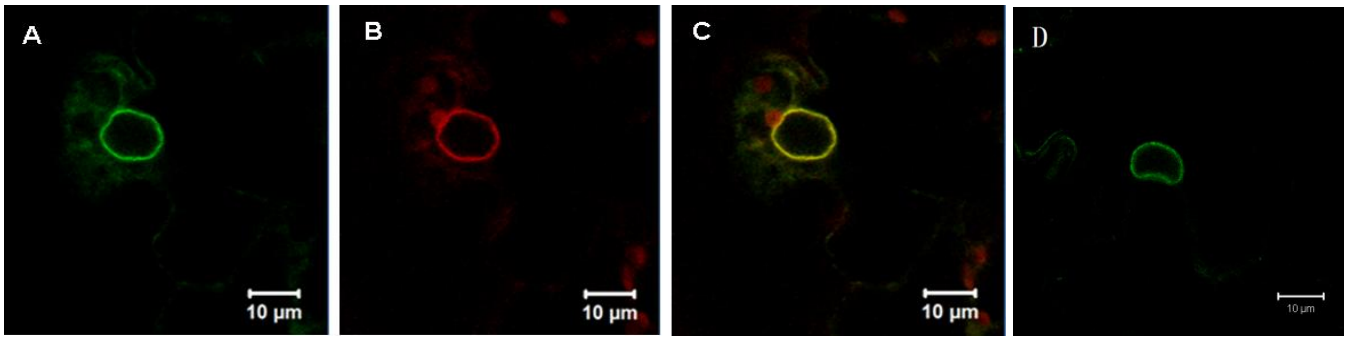

Figure 2. Subcellular localization of AtNEA1 transiently expressed in *N. benthamiana* epidermal leaf cells. Confocal laser scanning microscopy images of representative *N. benthamiana* cells showing fluorescence of (A) AtSUN1-CFP marker protein, (B) AtNEA1-YFP. YFP (530-600 nm) and CFP (475-525 nm) channels were scanned simultaneously. (C) Merged images of (A) and (B). The excitation wavelengths were 514 nm for YFP and 458 nm for CFP. The same information is gained by YFP-AtNEA1 transiently expression. (D) YFP-AtNEA1. YFP (530-600 nm) and CFP (475-525 nm) channels were scanned simultaneously.

Table 1. Fluorescence resonance energy transfer (FRET) efficiencies statistic data.

Co expressed proteins	E_f (%)	Control E_f (%)
CFP-AtSUN1+YFP-AtNEA1	2.62±3.89	2.82±3.89
AtSUN1-CFP+YFP-AtNEA1	3.20±5.12	1.45±3.78
CFP-AtSUN2+YFP-AtNEA1	4.04±7.91	3.81±6.18
AtSUN2-CFP+YFP-AtNEA1	3.24±6.01	3.78±7.84

crushed and the proteins were extracted. The extracted proteins were separated by Triton X-114 bi-phase: aqueous phase and detergent phase. A single band of YFP-AtNEA1 and a single band of AtNEA1-YFP in aqueous lanes on Cy5 stained Western blots indicate AtNEA1 as a soluble protein, rather than a membrane intrinsic protein (insoluble) (Figure 3A and 3B). GFP-CXN (calnexin) (insoluble) and GFP-HDEL (soluble) were used as the markers.

Intracellular localizations of AtNEA1 mutants

By applying SOE PCR methods (Dahm and Jennewein, 2010), putative NLS, coiled coil 1, coiled coil 2 and transmembrane domains were deleted respectively. The mutants were fused into YFP- tagged vectors and transiently expressed in *N. benthamiana* and observed by confocal microscopy at YFP channel settings described earlier. The mutant of NLS deletion (AtNEA1ΔNLS)'s subcellular localization appeared to be both cytoplasmic and nucleoplasmic, indicating NLS is not essential for AtNEA1 to enter nuclei but can strongly increase the transport efficiency, at the same time NLS participates in anchoring AtNEA1 to the INM. The mutants of coiled coil 1 domain deletion (AtNEA1ΔCC1) and coiled coil 2 domain deletion (AtNEA1ΔCC2)'s subcellular localizations both appeared to be nucleoplasmic, indicating both coiled coiled coil 1 domain and coiled coil 2 domain participate in anchoring AtNEA1 to INM. The mutant of putative transmembrane domain truncation (the last 2 amino acids after the putative transmembrane domain were removed)'s subcellular localization appeared to be NE periphery, indicating putative transmembrane domain is not functional. Figure 4A, B, C and D show the subcellular localizations of AtNEA1 mutants.

The sub-cellular localisations of fluorescence tagged AtNEA1 in BY-2 cells

The sub-cellular localisations of both AtNEA1-YFP and YFP-AtNEA1 were observed to be at the nuclear envelope periphery. This observation further confirmed the previous observation data that AtNEA1 is a nuclear envelope periphery localized protein. Also, the BY-2 cell study indicated the coherent information for sub-cellular localisation of AtNEA1-YFP and YFP-AtNEA1 in Arabidopsis thaliana in addition to the sub-cellular locaisation of AtNEA1 in transient transformed *Nicotiana tabacum* (Cv. Petit Havana SR1) (Figure 5).

Characterisation of T-DNA knockouts

The SAIL_SALK T-DNA insertion lines of At3g05830 as well as the wild type (WT) line were grown on agar plates (the SAIL_SALK T-DNA lines grew in agar plates with and without the antibiotic kanamycin) and the morphology of the seedlings was observed. The SAIL line grew on agar plates with and without kanamycin, suggesting the SAIL T-DNA insertion has silenced the kanamycin resistance gene.

The growth and morphology of the shoot apex, cotyledons, hypocotyl and roots did not show any significant differences (Figure 6). The T-DNA SAIL_SALK insertions were screened by genome sequence. In order to determine

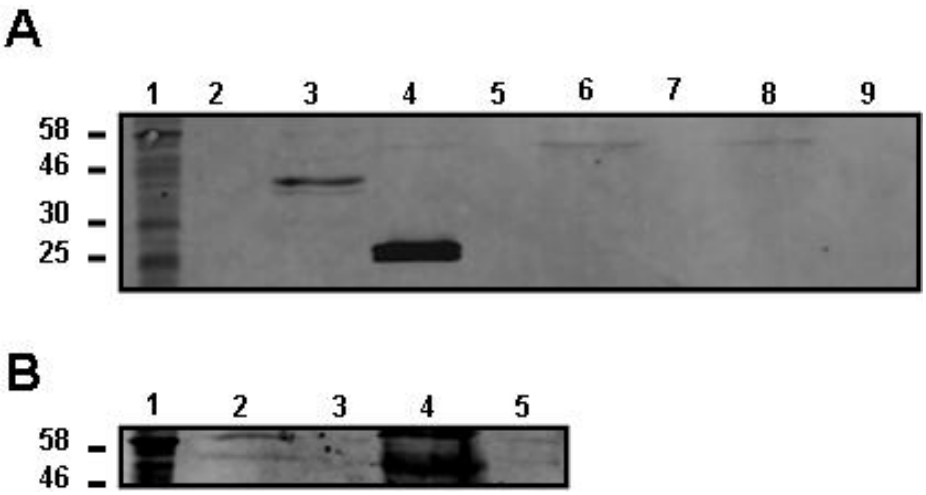

Figure 3. Solubility test of AtNEA1. *A. tumefaciens* (GV3101) was transformed with YFP- tagged AtNEA1, as well as GFP-CXN (calnexin) and GFP-HDEL as the markers. Extracts from the transformed *N. benthamiana* cells were phased by Triton X-114 separation and analyzed by Western blotting. (A) Western blotting of transformed *N. benthamiana* leaf cell extracts using anti-GFP antibodies (abcam, Cambridge, UK). Lane 1, protein marker with molecular masses to the left in kDa; lane 2, cell lysate from GFP-CXN transformed leaf in TX-114 aqueous phase; lane 3, cell lysate from GFP-CXN transformed leaf in TX-114 detergent phase; lane 4, cell lysate from GFP-HDEL transformed leaf in TX-114 aqueous phase; lane 5, cell lysate from GFP-HDEL transformed leaf in TX-114 detergent phase; lane 6, cell lysate from YFP-AtNEA1 transformed leaf in TX-114 aqueous phase; lane 7, cell lysate from YFP-AtNEA1 transformed leaf in TX-114 detergent phase; lane 8, cell lysate from AtNEA1-YFP transformed leaf in TX-114 aqueous phase; lane 9, cell lysate from AtNEA1-YFP transformed leaf in TX-114 detergent phase. (B) Solubility was confirmed by Western blotting using newly raised anti-AtNEA1 antpeptides (Genosphere Biotech, Paris, France). Lane 1, protein marker with molecular masses to the left in kDa; lane 2, cell lysate from YFP-AtNEA1 transformed leaf in TX-114 aqueous phase; lane 3, cell lysate from YFP-AtNEA1 transformed leaf in TX-114 detergent phasse; lane 4, cell lysate from AtNEA1-YFP transformed leaf in TX-114 aqueous phase; lane 5, cell lysate from AtNEA1-YFP transformed leaf in TX-114 detergent phase.

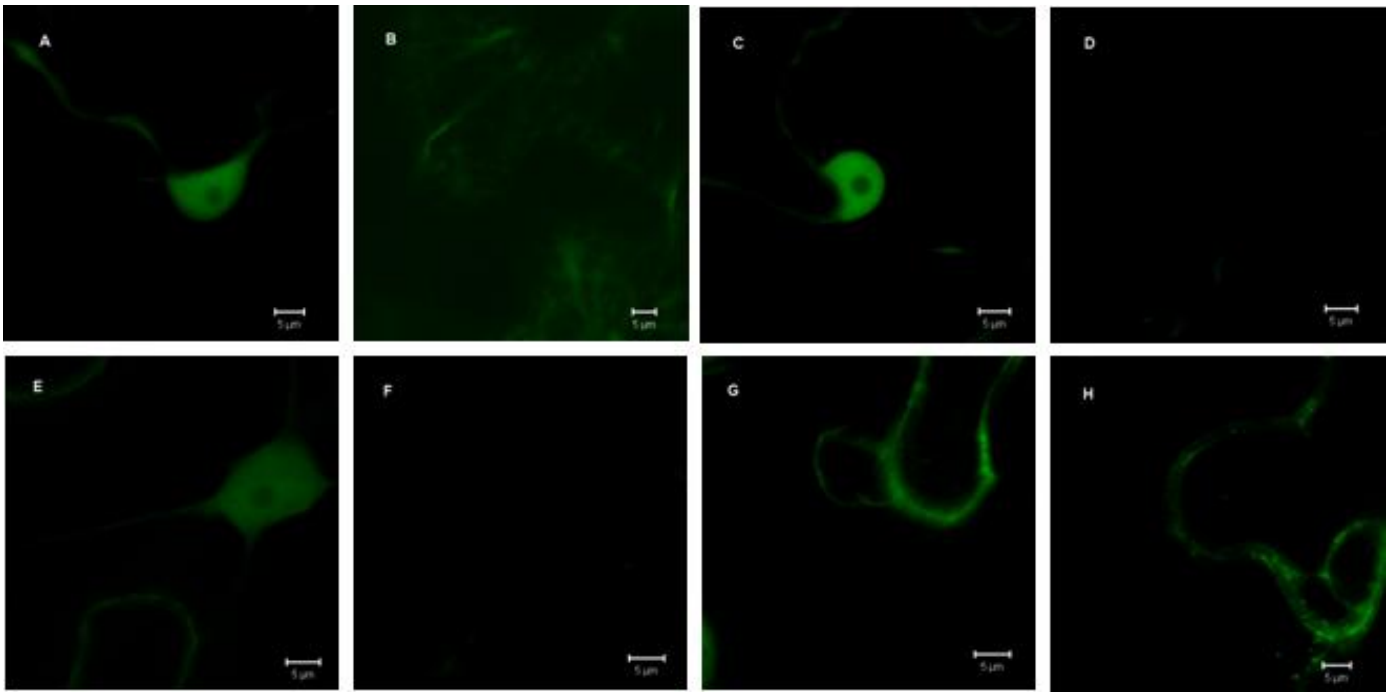

Figure 4. Subcellular localization of AtNEA1 domain mutants transiently expressed in *N. benthamiana* epidermal leaf cells. A) Confocal laser scanning microscopy images of representative *N. benthamiana* cells showing fluorescence of (A) AtNEA1ΔNLS-YFP in nucleoplasmic focus. (B) AtNEA1ΔNLS-YFP in cytoplasmic focus. (C) AtNEA1ΔCC1-YFP in nucleoplasmic focus. (D) AtNEA1ΔCC1-YFP in cytoplasmic focus. (E) AtNEA1ΔCC2-YFP in nucleoplasmic focus. (F) AtNEA1ΔCC2-YFP in cytoplasmic focus. (G) YFP-AtNEA1ΔTM. (H) AtNEA1ΔTM-YFP. YFP (530-600 nm) channels were scanned simultaneously. The excitation wavelengths were 514 nm for YFP. The same information is gained by YFP-AtNEA1ΔNLS, YFP-AtNEA1ΔCC1, YFP-AtNEA1ΔCC2 and YFP-AtNEA1ΔTM transiently expressed.

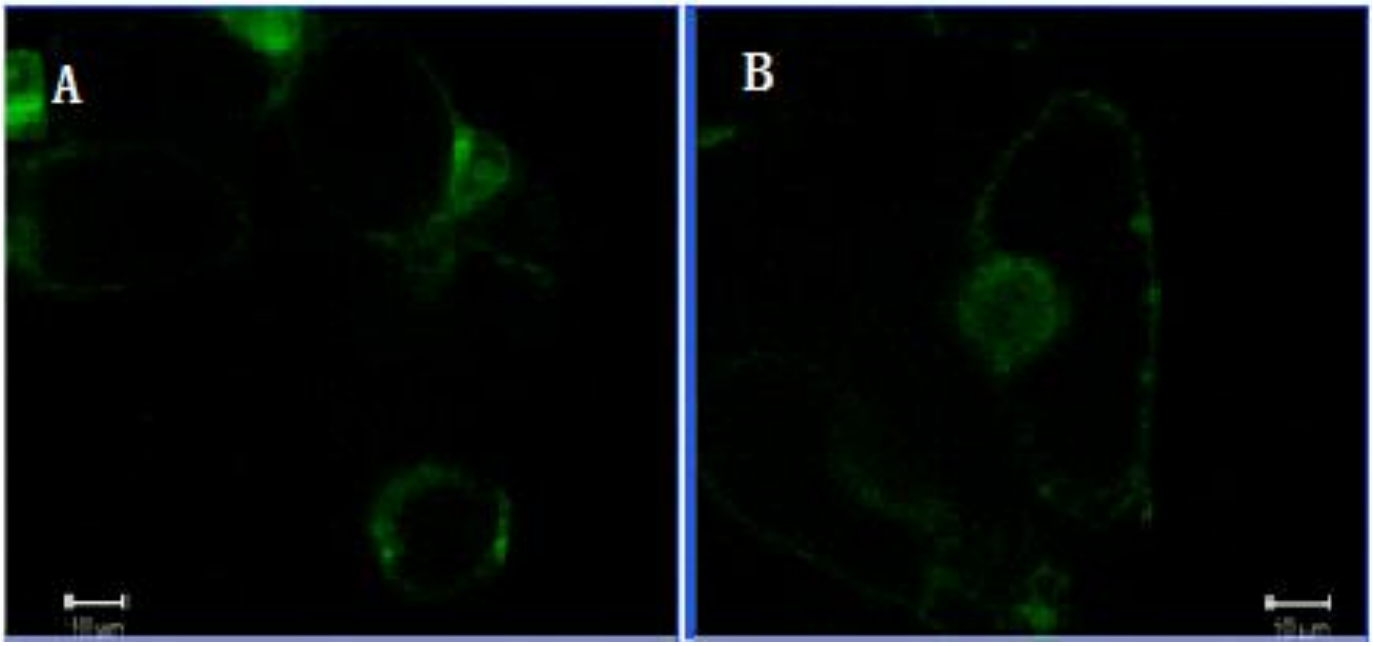

Figure 5. The sub-cellular localisations of YFP-AtNEA1 and AtNEA1-YFP in BY-2 cells. A. Confocal laser scanning microscopy images of representative BY-2 cells showing fluorescence of (A)YFP-AtNEA1 in nuclear envelope periphery focus, (B) AtNEA1-YFP in nuclear envelope periphery focus channels were scanned simultaneously. The excitation wavelengths were 514 nm for YFP.

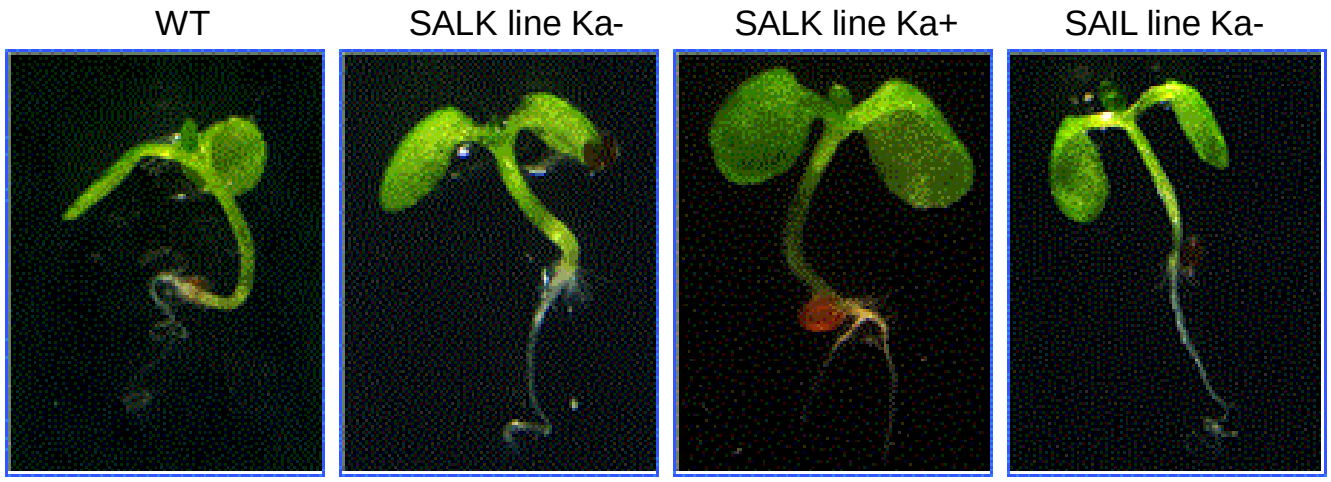

Figure 6. Comparison of the seedlings morphology of *Arabidopsis* wild type, SALK line (without kanamycin), SALK line (with kanamycin) and SAIL line (without kanamycin). SALK (N521615) and SAIL (N837770) lines were provided by NASC, Nottingham, UK.

the size of the nucleus of T-DNA SAIL_SALK lines as well as wild type (WT), leaf pieces were stained with ethidium bromide (EB) and scanned by confocal microscopy. The nucleus size was measured by LSM image browser software.

Samples (30) for each line were measured at the greatest diameter and the data was analyzed by F-test and t-test (P>0.05). The SAIL (N837770) line and the SALK (N521615) line were not significantly different from the wild type (WT). The images of nucleus are shown in Figure 7 and the statistical analysis is shown in Table 2.

DISCUSSION

Bioinformatics of AtNEA1

AtNEA1 (At3g05830) has a predicted NLS sequence at

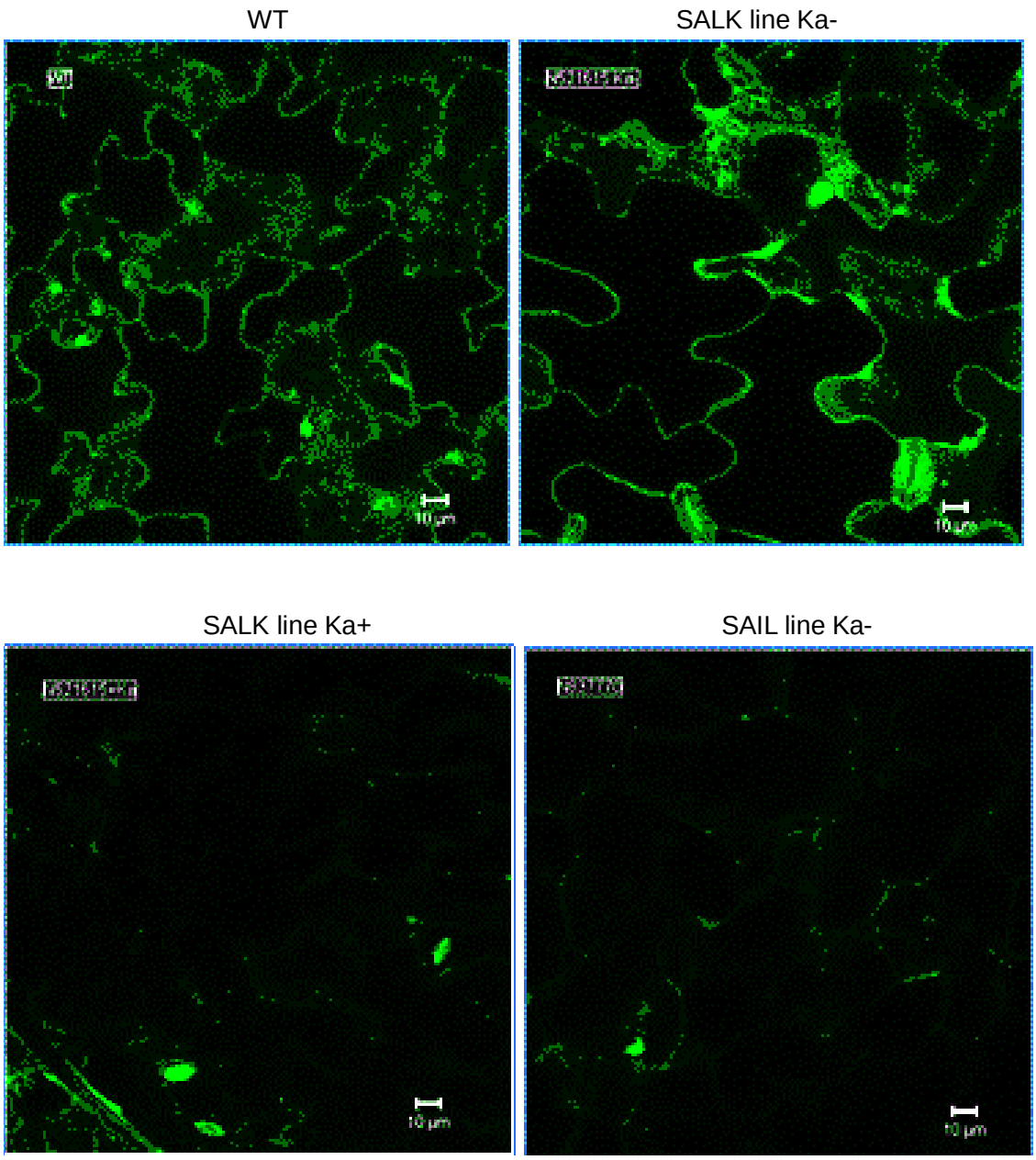

Figure 7. The nucleus images of *Arabidopsis* wild type, T-DNA SAIL (N837770) line (in plate without kanamycin), SALK (N521615) line (in plate without kanamycin), SALK (N521615) line (in plate with kanamycin). SALK (N521615) and SAIL (N837770) lines were provided by NASC, Nottingham, UK. YFP (shown in green) was visualised using an argon laser at 514 nm wavelength. Images were taken with ×63 objective oil immersed lens at various zoom levels. Leaf pieces were stained with ethidium bromide (EB) and scanned by confocal microscopy.

Table 2. The nucleus size measurements of *Arabidopsis* wild type, T-DNA SAIL (N837770) line (in plate without kanamycin), SALK (N521615) line (in plate without kanamycin), SALK (N521615) line (in plate with kanamycin).

Arabidopsis lines	Nucleus size (the greatest diameter of nucelus) unit: μm	Standard deviation
Wild type	7.60	±1.89
SALK line (Ka+)	7.13	±1.06
SALK line (Ka-)	8.27	±1.47
SAIL line (Ka-)	7.19	1.30

SALK (N521615) and SAIL (N837770) lines were provided by NASC, Nottingham, UK.

the N-terminal (from 60 ~ 75 aa) and a predicted transmembrane domain at the C-terminal (from 321 ~ 334 aa) and two coiled coil domains (120 ~ 180 aa and from 238 ~ 306 aa) (SMART: smart.embl-heidelberg.de/; PredictNLS: www.predictprotein.org/cgi/var/nair/resonline.pl). The NCBI BLAST (http://blast.ncbi.nlm.nih.gov/Blast.cgi) homology protocol was applied to the sequence of At3g05830 against proteins in the *Arabidopsis thaliana* database (TAIR). At5g26770 was indicated to show 81% homology (E value: $2e^{-47}$) with it. It can be inferred that At5g26770 shares similarities with At3g05830 in terms of function and structure (BP-NLS, coiled coil domain and TM domain are conserved domains for At3g05830 and At5g26770). Therefore, At5g26770 may have close function similarity with At3g05830 or it may be a functional substitute of At3g05830. There are no characterised animal proteins that show homology with At3g05830. This implies At3g05830 is a plant exclusive protein. The expression pattern for *A. thaliana* indicates At3g05830 is relative highly expressed in Arabidopsis embryo, micropylar endosperm, peripheral endosperm, chalazal endosperm, lateral root cap, general seed coat and suspensor. The expression pattern implies a role for At3g05830 in development. The richness of At3g05830 in endosperm implies At3g05830 may function in nutrition of the embryo or release of storage reserves. The stimuli map of At3g05830 (data not shown) shows At3g05830 is stably expressed under various physical or chemical stresses. The data indicates the expression of At3g05830 is ubiquitous in Arabidopsis thaliana and implies At3g05830 has an essential role in *A. thaliana*.

The localization information together indicates: AtNEA1 (At3g05830) is a plant nuclear envelope associated protein; the putative NLS is not essential for At3g05830 to enter nuclei, but can strongly increase the efficiency of transport; the putative NLS also participates in anchoring At3g05830 to nuclear envelope periphery; both the putative coiled coil domain 1 and coiled coil domain 2 participate in anchoring At3g05830 to the nuclear envelope periphery; the putative transmembrane domain appeared to be non-functional. The integrity and stability of the YFP constructs were confirmed by expression followed by western blotting against anti FP antibodies, where proteins of appropriate Mr were detected.

Properties of AtNEA1

At3g05830 was observed to be localized at tobacco leaf cell nuclear envelope periphery by confocal microscopy in transient expression. It was also observed to be co-localized with AtSUN1 and AtSUN2 at the same location in transient expression. The putative NLS, coiled coil domain 1, coiled coil domain 2 and putative transmembrane domain were deleted or truncated respectively. The subcellular localization of AtNEA1ΔNLS appeared to be both nucleoplasmic and cytoplasmic. The subcellular localization of AtNEA1ΔCC1 appeared to be nucleoplasmic. The subcellular localization of AtNEA1ΔCC2 appeared to be nucleoplasmic. The subcellular localization of AtNEA1ΔTM appeared to be nuclear periphery. In the Triton X-114 solubility study, At3g05830 was shown to be in the aqueous phase (soluble phase) of Triton X-114 phase partition.

In combination with the results from domain mutant study, At3g05830 is predicted to be a free-diffuse nucleoplasmic protein, which is anchoring to the INM by interacting with an unknown INM-intrinsic protein. The NLS sequence and two coiled coil domains are all taking part in forming the interaction structure for AtNEA1 with its INM interaction partner. The protein itself can diffuse through the NPC, but the NLS can also be recognized by importins and directed through NPC.

According to the FRET data statistical analysis (Table 1), the efficiencies Ef (Ef is the quantum yield of the energy transfer transition) of CFP did not increase after the bleach of YFP. Therefore, it was not indicated that At3g05830 was interacting with AtSUN1 or AtSUN2; however, FRET does not prove the absence of interaction *in vivo*, as other factors, like the effect of the presence of the fluorescent protein groups, could prevent co-localisation. Study of the phenotype of the Arabidopsis T-DNA lines of AtNEA1 (At3g05830) (SAIL and SALK) did not reveal observable differences in comparison with wild type for any of the parameters measured. Hence, little information can be acquired about the potential function of At3g05830 in terms of affecting Arabidopsis morphology. The nucleus size comparison of Arabidopsis T-DNA lines of At3g05830 (SAIL and SALK) did not show statistically significant differences in comparison with wild type. Hence, little information can be acquired about the potential function of At3g05830 in terms of affecting the size of Arabidopsis cell nucleus. The presence of the T-DNA lines genome insertion was confirmed and the T-DNA lines were proved as homozygous. Absence of identified phenotype therefore may be because another gene, or a homologue, is present which replaces At3g05830 function. One candidate for this could be At5g26770, which shows structural similarity.

AtNEA1 is a novel plant nuclear envelope associated protein and was shown to contain a NLS and two coiled coil domains. Results suggested that a hydophobic domain at the C-terminus was not as predicted a transmembrane domain. Deletion of the coiled coil domains, however, resulted in altered localization and lack of interaction with the NE. The NLS appears to increase localization of the protein to the nucleus. No homologues for At3g05830 were shown in animals or yeasts, though plants appear to have once copy of At3g05830 and one of its putative homologue At5g26770. When At3g05830 function was investigated using SALK and SAIL T-DNA intertion mutants, no phenotype was detected, in morphology, development on size of nucleus.

It is therefore possible to assume AtNEA1 is a functionally substitute of At5g26770 in *A. thalian* but further functions and roles need to be explored.

ACKNOWLEDGEMENT

I thank the Oxford Brookes University for providing support for this study.

REFERENCES

Andreasson C, Ljungdahl PO (2002). Receptor-mediated endoproteolytic activation of two transcription factors in yeast. Genes Dev. 16:3158-3172.

Blumenthal SS, Clark GB, Roux SJ (2004). Biochemical and immunological characterization of pea nuclear intermediate filament proteins. Planta 218:965-975.

Bordier C (1981) Phase separation of integral membrane proteins in Triton X-114 solution. J. Biol. Chem. 256:1604-1607.

Broers JL, Machiels BM, van Eys GJ, Kuijpers HJ, Manders EM, van Driel R, Ramaekers FC (1999). Dynamics of the nuclear lamina as monitored by GFP-tagged A-type lamins. J. Cell Sci. 112 (20):3463-3475.

Buendia B, Courvalin JC (1997). Domain-specific disassembly and reassembly of nuclear membranes during mitosis. Exp. Cell Res. 230:133-144.

Caorsi V, Ushakov DS, West TG, Setta-Kaffetzi N, Ferenczi MA (2011) FRET characterisation for cross-bridge dynamics in single-skinned rigor muscle fibres. Eur. Biophys. J. 40:13-27.

Chi YH, Haller K, Peloponese JM, Jr, Jeang KT (2007). Histone acetyltransferase hALP and nuclear membrane protein hsSUN1 function in de-condensation of mitotic chromosomes. J. Biol. Chem. 282:27447-27458.

Chikashige Y, Tsutsumi C, Yamane M, Okamasa K, Haraguchi T, Hiraoka Y (2006). Meiotic proteins bqt1 and bqt2 tether telomeres to form the bouquet arrangement of chromosomes. Cell 125:59-69.

Chu A, Rassadi R, Stochaj U (1998). Velcro in the nuclear envelope: LBR and LAPs. FEBS Lett. 441:165-169.

Crisp M, Burke B (2008). The nuclear envelope as an integrator of nuclear and cytoplasmic architecture. FEBS Lett. 582:2023-2032. doi:10.1016/j.febslet.2008.05.001.

Crisp M, Liu Q, Roux K, Rattner JB, Shanahan C, Burke B, Stahl PD, Hodzic D (2006) Coupling of the nucleus and cytoplasm: role of the LINC complex. J. Cell Biol. 172:41-53.

Dahm P, Jennewein S (2010). Introduction of the early pathway to taxol biosynthesis in yeast by means of biosynthetic gene cluster construction using SOE-PCR and homologous recombination. Methods Mol. Biol. 643:145-163.

D'Angelo MA, Hetzer MW (2006). The role of the nuclear envelope in cellular organization. Cell Mol. Life Sci. 63:316-332.

Dittmer TA, Stacey NJ, Sugimoto-Shirasu K, Richards EJ (2007). LITTLE NUCLEI genes affecting nuclear morphology in Arabidopsis thaliana. Plant Cell 19:2793-2803.

Forsberg H, Ljungdahl PO (2001). Genetic and biochemical analysis of the yeast plasma membrane Ssy1p-Ptr3p-Ssy5p sensor of extracellular amino acids. Mol. Cell Biol. 21:814-826.

Gindullis F, Peffer NJ, Meier I (1999). MAF1, a novel plant protein interacting with matrix attachment region binding protein MFP1, is located at the nuclear envelope. Plant Cell 11:1755-1768.

Gindullis F, Rose A, Patel S, Meier I (2002). Four signature motifs define the first class of structurally related large coiled-coil proteins in plants. BMC Genomics 3:9.

Goldberg M, Harel A, Gruenbaum Y (1999). The nuclear lamina: molecular organization and interaction with chromatin. Crit. Rev. Eukaryot Gene Expr. 9:285-293.

Graumann K, Evans DE (2010). The plant nuclear envelope in focus. Biochem. Soc. Trans. 38:307-311.

Graumann K, Runions J, Evans DE (2010) Characterization of SUN-domain proteins at the higher plant nuclear envelope. Plant J. 61:134-144.

Gruenbaum Y, Margalit A, Goldman RD, Shumaker DK, Wilson KL (2005). The nuclear lamina comes of age. Nat. Rev. Mol. Cell Biol. 6:21-31.

Haque F, Lloyd DJ, Smallwood DT, Dent CL, Shanahan CM, Fry AM, Trembath RC, Shackleton S (2006). SUN1 interacts with nuclear lamin A and cytoplasmic nesprins to provide a physical connection between the nuclear lamina and the cytoskeleton. Mol. Cell Biol. 26:3738-3751.

Haraguchi T, Holaska JM, Yamane M, Koujin T, Hashiguchi N, Mori C, Wilson KL, Hiraoka, Y (2004). Emerin binding to Btf, a death-promoting transcriptional repressor, is disrupted by a missense mutation that causes Emery-Dreifuss muscular dystrophy. Eur. J. Biochem. 271:1035-1045.

Haraguchi T, Koujin T, Segura-Totten M, Lee KK, Matsuoka Y, Yoneda Y, Wilson KL, Hiraoka Y (2001). BAF is required for emerin assembly into the reforming nuclear envelope. J. Cell Sci. 114:4575-4585.

Herrmann H, Aebi U (2004). Intermediate filaments: molecular structure, assembly mechanism, and integration into functionally distinct intracellular Scaffolds. Annu. Rev. Biochem. 73:749-789.

Hodzic DM, Yeater DB, Bengtsson L, Otto H, Stahl PD (2004). Sun2 is a novel mammalian inner nuclear membrane protein. J. Biol. Chem. 279:25805-25812.

Hoffmann K, Dreger CK, Olins AL, Olins DE, Shultz LD, Lucke B, Karl H, Kaps R, Muller D, Vaya A, Aznar J, Ware RE, Sotelo Cruz N, Lindner TH, Herrmann H, Reis A, Sperling K (2002). Mutations in the gene encoding the lamin B receptor produce an altered nuclear morphology in granulocytes (Pelger-Huet anomaly). Nat. Genet. 31:410-414.

Holaska JM, Lee KK, Kowalski AK, Wilson KL (2003). Transcriptional repressor germ cell-less (GCL) and barrier to autointegration factor (BAF) compete for binding to emerin in vitro. J. Biol. Chem. 278: 6969-6975.

Kemp CA, Song MH, Addepalli MK, Hunter G, O'Connell K (2007). Suppressors of zyg-1 define regulators of centrosome duplication and nuclear association in Caenorhabditis elegans. Genetics 176:95-113.

Kleffmann T, Hirsch-Hoffmann M, Gruissem W, Baginsky S (2006). plprot: A comprehensive proteome database for different plastid types. Plant Cell Physiol. 47:432-436.

Koncz C, Schell J (1986) The promoter of TL-DNA gene 5 controls the tissue-specific expression of chimaeric genes carried by a novel type of Agrobacterium binary vector. Mol. Gen. Genet. 204:383-396.

Lassoued K, Danon F, Brouet JC (1991). Human autoantibodies to lamin B receptor are also anti-idiotypic to certain anti-lamin B antibodies. Eur. J. Immunol. 21:1959-1962.

Li H, Roux SJ (1992). Casein kinase II protein kinase is bound to lamina-matrix and phosphorylates lamin-like protein in isolated pea nuclei. Proc. Natl. Acad. Sci. USA 89:8434-8438.

Lin F, Morrison JM, Wu W, Worman HJ (2005). MAN1, an integral protein of the inner nuclear membrane, binds Smad2 and Smad3 and antagonizes transforming growth factor-beta signaling. Hum. Mol. Genet. 14:437-445.

Lin F, Noyer CM, Ye Q, Courvalin JC, Worman HJ (1996). Autoantibodies from patients with primary biliary cirrhosis recognize a region within the nucleoplasmic domain of inner nuclear membrane protein LBR. Hepatology 23:57-61.

Massague J, Seoane J, Wotton D (2005). Smad transcription factor. Genes Dev. 19:2783-2810.

Masuda K, Xu ZJ, Takahashi S, Ito A, Ono M, Nomura K, Inoue M (1997). Peripheral framework of carrot cell nucleus contains a novel protein predicted to exhibit a long alpha-helical domain. Exp. Cell Res. 232:173-181.

McNulty AK, Saunders MJ (1992). Purification and immunological detection of pea nuclear intermediate filaments: evidence for plant nuclear lamins. J. Cell Sci. 103(2):407-414.

Meier I, Phelan T, Gruissem W, Spiker S, Schneider D (1996). MFP1, a novel plant filament-like protein with affinity for matrix attachment region DNA. Plant Cell 8:2105-2115.

Meier I, Zhou X, Brkljacic J, Rose A, Zhao Q, Xu XM (2010). Targeting proteins to the plant nuclear envelope. Biochem. Soc. Trans. 38:733-740.

Meier I (2001). The plant nuclear envelope. Cell Mol. Life Sci. 58:1774-1780.
Meier I (2007). Composition of the plant nuclear envelope: theme and variations. J. Exp. Bot. 58:27-34.
Moir RD, Spann TP (2001). The structure and function of nuclear lamins: implications for disease. Cell Mol. Life Sci. 58:1748-1757.
Morris GE. (2001). The role of the nuclear envelope in Emery-Dreifuss muscular dystrophy. Trends Mol. Med. 7:572-577.
Osada S, Ohmori SY, Taira M (2003). XMAN1, an inner nuclear membrane protein, antagonizes BMP signaling by interacting with Smad1 in Xenopus embryos. Development 130:1783-1794.
Patel S, Rose A, Meulia T, Dixit R, Cyr RJ, Meier I (2004). Arabidopsis WPP-domain proteins are developmentally associated with the nuclear envelope and promote cell division. Plant Cell 16:3260-3273.
Peiter E, Sun J, Heckmann AB, Venkateshwaran M, Riely BK, Otegui MS, Edwards A, Freshour G, Hahn MG, Cook DR, Sanders D, Oldroyd GE, Downie JA, Ane JM (2007). The Medicago truncatula DMI1 protein modulates cytosolic calcium signaling. Plant Physiol. 145:192-203.
Pendle AF, Clark GP, Boon R, Lewandowska D, Lam YW, Andersen J, Mann M, Lamond AI, Brown JW, Shaw PJ (2005). Proteomic analysis of the Arabidopsis nucleolus suggests novel nucleolar functions. Mol. Biol. Cell 16: 260-269.
Prokocimer M, Davidovich M, Nissim-Rafinia M, Wiesel-Motiuk N, Bar DZ, Barkan R, Meshorer E, Gruenbaum Y (2009). Nuclear lamins: key regulators of nuclear structure and activities. J. Cell Mol. Med. 13:1059-1085.
Pyrpasopoulou A, Meier J, Maison C, Simos G, Georgatos SD (1996). The lamin B receptor (LBR) provides essential chromatin docking sites at the nuclear envelope. EMBO J. 15:7108-7119.
Razafsky D, Hodzic D (2009) Bringing KASH under the SUN: the many faces of nucleo-cytoskeletal connections. J. Cell Biol. 186:461-472.
Riely BK, Lougnon G, Ane JM, Cook DR (2007). The symbiotic ion channel homolog DMI1 is localized in the nuclear membrane of Medicago truncatula roots. Plant J. 49:208-216.
Rose A, Gindullis F, Meier I (2003). A novel alpha-helical protein, specific to and highly conserved in plants, is associated with the nuclear matrix fraction. J. Exp. Bot. 54:1133-1141.
Rose A, Patel S, Meier I (2004). The plant nuclear envelope. Planta 218:327-336.
Starr DA (2009). A nuclear-envelope bridge positions nuclei and moves chromosomes. J Cell Sci. 122:577-586.
Stewart CL, Roux KJ, Burke B (2007). Blurring the boundary: the nuclear envelope extends its reach. Science 318:1408-1412.
Stuurman N, Heins S, Aebi U (1998). Nuclear lamins: their structure, assembly, and interactions. J. Struct. Biol. 122:42-66.
ten Dijke P, Hill CS (2004). New insights into TGF-beta-Smad signalling. Trends Biochem. Sci. 29:265-273.
Tomita K, Cooper JP (2006). The meiotic chromosomal bouquet: SUN collects flowers. Cell 125:19-21.
Tzur YB, Margalit A, Melamed-Book N, Gruenbaum Y (2006). Matefin/SUN-1 is a nuclear envelope receptor for CED-4 during Caenorhabditis elegans apoptosis. Proc. Natl. Acad. Sci. USA 103:13397-13402.
Vlcek S, Dechat T, Foisner R (2001). Nuclear envelope and nuclear matrix: interactions and dynamics. Cell Mol. Life Sci. 58:1758-1765.
Wang Q, Du X, Cai Z, Greene MI (2006). Characterization of the structures involved in localization of the SUN proteins to the nuclear envelope and the centrosome. DNA Cell Biol. 25:554-562.
Waterham HR, Koster J, Mooyer P, Noort GG, Kelley RI, Wilcox WR, Wanders RJ, Hennekam RC, Oosterwijk JC (2003). Autosomal recessive HEM/Greenberg skeletal dysplasia is caused by 3 beta-hydroxysterol delta 14-reductase deficiency due to mutations in the lamin B receptor gene. Am. J. Hum. Genet. 72:1013-1017.
Wilhelmsen K, Ketema M, Truong H, Sonnenberg A (2006) KASH-domain proteins in nuclear migration, anchorage and other processes. J. Cell Sci. 119:5021-5029.
Wilkinson FL, Holaska JM, Zhang Z, Sharma A, Manilal S, Holt I, Stamm S, Wilson KL, Morris GE (2003). Emerin interacts in vitro with the splicing-associated factor, YT521-B. Eur. J. Biochem. 270:2459-2466.
Worman HJ, Yuan J, Blobel G, Georgatos SD (1988). A lamin B receptor in the nuclear envelope. Proc. Natl. Acad. Sci. USA 85:8531-8534.
Xiong TC, Bourque S, Mazars C, Pugin A, Ranjeva R (2006). [Cytosolic and nuclear calcium signalling in plants reply to biotic and abiotic stimuli]. Med. Sci. (Paris) 22:1025-1028.
Xu XM, Meier I (2008). The nuclear pore comes to the fore. Trends Plant Sci. 13:20-27.
Ye Q, Callebaut I, Pezhman A, Courvalin JC, Worman HJ (1997). Domain-specific interactions of human HP1-type chromodomain proteins and inner nuclear membrane protein LBR. J. Biol. Chem. 272:14983-14989.
Zhao Q, Brkljacic J, Meier I (2008). Two distinct interacting classes of nuclear envelope-associated coiled-coil proteins are required for the tissue-specific nuclear envelope targeting of Arabidopsis RanGAP. Plant Cell 20:1639-1651.